Bubbly Turbulent Drag Reduction Is a Boundary Layer Effect

Thomas H. van den Berg,[1] Dennis P. M. van Gils,[1] Daniel P. Lathrop,[2] and Detlef Lohse[1,*]

[1]*Department of Applied Physics, IMPACT, and J. M. Burgers Center for Fluid Dynamics, Physics of Fluids Group,
University of Twente, P.O. Box 217, 7500 AE Enschede, Netherlands*
[2]*Institute for Research in Electronics and Applied Physics, University of Maryland, College Park, Maryland, USA*

In turbulent Taylor-Couette flow, the injection of bubbles reduces the overall drag. On the other hand, rough walls enhance the overall drag. In this work, we inject bubbles into turbulent Taylor-Couette flow with rough walls (with a Reynolds number up to 4×10^5), finding an enhancement of the dimensionless drag as compared to the case without bubbles. The dimensional drag is unchanged. As in the rough-wall case no smooth boundary layers can develop, the results demonstrate that bubbly drag reduction is a pure boundary layer effect.

PACS numbers: 47.27.−i

Turbulent drag reduction can be achieved by polymers [1–5], by bubbles [5–12], or by a combination of both [13]. The phenomenon has huge potential for applications in the naval transport sector [14]. Even a small reduction of a few percent on the fuel consumption of ships means a considerable annual saving. One drag reduction method is to reduce the skin friction through microbubble injection at the ship's hull. Using this, a research team in Japan has found drag reduction on an experimental ship, the Seiun-Maru, of up to 5% [15]. An U.S. research team achieved reductions of 5%–15% with a catamaran supplied with a microbubble drag reduction system [16].

A generally accepted explanation of the effect is lacking. Several theories are competing: Based on numerical simulations, Ferrante and Elghobashi [17] argue that the microbubbles in a spatially developing turbulent boundary layer push the developing streamwise vortices away from the wall, leading to less dissipation in the boundary layer. Numerical simulations by Lu, Fernandez, and Tryggvason [18] show that deformable bubbles lead to a significant reduction of the drag by the suppression of streamwise vorticity. Van den Berg *et al.* [6] show that both mechanisms contribute, though the deformability of the bubbles seems to be of main importance, leading to stronger drag reduction. Lo, L'vov, and Procaccia [19] conclude that bubble volume oscillations and, thus, the compressibility of the bubble-water mixture play an important role for the drag reduction.

In this Letter, we investigate the effect of the wall roughness on bubbly drag reduction: first, because for practical applications rough walls are more realistic than smooth ones; second, in order to get more insight into the mechanism of bubbly drag reduction; and, in particular, to probe whether boundary layer (BL) effects play a role. Rough walls drastically modify the dynamics in the laminar BLs and trigger the development of turbulent BLs. Indeed, by roughening the walls in a single-phase flow Taylor-Couette setup, the overall drag could be increased by a factor of 50 [20,21]. Moreover, the drag scales more

steeply with the Reynolds number as compared to the smooth-wall case [20,21], in coherence with what one would expect when transferring the ideas of the unifying scaling theory for thermal convection [22] to the Taylor-Couette case [23].

The effect of bubbles on the drag within a turbulent water tunnel with rough walls has been examined in Ref. [24]. In these experiments, the drag force was directly measured with a drag balance, as a function of the downstream position and of the (injected) gas flow rate. In spite of the wall roughness, the addition of bubbles reduced the drag, similarly as the addition of polymers reduced the drag in such water tunnel experiments [24,25]. In these experiments [24,25], wavy structures or grits were attached to the surfaces of the walls. In the rough-wall case, the drag reduction effect of the polymers was even stronger than in the smooth-wall case, presumably because of the higher absolute drag for the rough-wall case [25]. In contrast, Cadot, Bonn, and Douady [26] did not find any polymeric drag reduction for *inertially forced* (with baffles) turbulence. They concluded that the polymeric drag reduction effect observed in the smooth-wall case is related solely to a diminution of the dissipation in the viscous boundary layer where most of the energy is dissipated. This is consistent with the present theoretical understanding of polymeric drag reduction; see, e.g., Refs. [4,27] and references therein.

To measure the potential drag reduction effect of bubbles in turbulence in a system with rough walls, we again choose the Taylor-Couette geometry, just as we did in Ref. [20] for the effect of rough walls only and in Ref. [6] for the effect of bubbles only. The advantage of the Taylor-Couette system is that it is *closed,* which makes it possible to deduce the overall dissipation rate ϵ from the well-controlled energy input rate determined by the torque. Moreover, statistically stationary states are easy to achieve. Thus, by measuring the torque on the inner cylinder (rotating with fixed angular velocity Ω), the total energy dissipation rate of the flow can be deduced, which in turn is a

measure of the drag:

$$\epsilon = \frac{T\Omega}{\pi\rho L(b^2 - a^2)} = \frac{\nu^2 G\Omega}{\pi(b^2 - a^2)}. \qquad (1)$$

Here T is the torque, $G = T/\rho\nu^2 L$ is its nondimensionalized form, ρ is the density of the liquid, and ν is the kinematic viscosity. The height of the cylinder is L, and the inner and outer radii are a and b, respectively. The drag coefficient c_ϵ follows from nondimensionalization:

$$c_\epsilon = \frac{\epsilon(b - a)}{\Omega^3 a^3} = \frac{T}{\pi\rho L\Omega^2 a^3(b + a)}. \qquad (2)$$

The Taylor-Couette setup used for these experiments is described in detail in Refs. [6,20,28]. Here we only briefly summarize its specifications and refer to the mentioned papers for more information. The setup has an inner cylinder with radius $a = 16$ cm and an outer cylinder with radius $b = 22$ cm; the liquid-containing gap is thus 6 cm. The outer cylinder is stationary; the inner one can rotate to frequencies up to 16 Hz, resulting in a maximum Re $\approx 10^6$ for the single-phase water case. The total length is $L = 69.5$ cm, resulting in an aspect ratio of $\Gamma = L/(b - a) = 11.6$. To minimize the effects of the top and bottom boundaries, the inner cylinder consists of three parts, with a measuring section in the middle. The length of this section is 40 cm. It is attached to the inner shaft by low friction bearings. The actual torque on this part is measured by means of a load cell and strain gauges, which are measured by means of a lock-in amplifier. The top and bottom sections of the fluid volume serve as heat sinks in order to maintain a constant temperature of the working liquid. In this way, we were able to keep the temperature constant within a tenth of a degree. Therefore, we assume the dynamic viscosity and the density to remain constant. In the experiments with rough walls, the roughening was achieved by attaching 16 square Perspex rods (thickness 3 mm) equally spaced in azimuthal angle on the inner and outer cylinders, as in Refs. [20,21]. Note that in the rough-wall case the Taylor-Reynolds number is considerably larger than in the smooth-wall case, due to the enhanced forcing [20,21,26].

The air bubbles are injected into the turbulent flow through eight needles located at the bottom of the outer cylinder. The void fraction α was estimated by measuring the excess volume pushed out of the system because of the added gas as in Ref. [6]. The bubble size is dictated by the strength of the shear and is typically in the range of 2–0.5 mm [29]. The boundary layer inner length scale is significantly smaller, $y_0 = \nu/u_* \approx 3$ μm, with $u_* = \sqrt{\tau_w/\rho}$ and the shear stress τ_w being estimated as [28] $\tau_w = T/\pi a^2 L$.

Because of centrifugal forces, the air bubbles tend to accumulate near the inner cylinder, which eventually

would lead to a decoupling of the working liquid from the inner cylinder. However, when limiting the void fractions to values of up to 8%, the decoupling can be prevented.

When injecting bubbles into the flow, the kinematic viscosity and density are changed. It is $\rho = \rho_0(1 - \alpha)$, and the kinematic viscosity for a bubbly liquid is assumed to obey [30]

$$\nu = \nu_0(1 + \tfrac{5}{2}\alpha), \qquad (3)$$

where $\nu_0 = \nu(\alpha = 0)$. Another reason to limit ourselves to low overall gas fractions of up to 8% is that relation (3) becomes more and more questionable for larger gas fractions (see, e.g., Ref. [31])—but note that the *local* gas concentration can be higher than 8% due to bubble accumulation in the vortices. The flow Reynolds number is defined with the viscosity of the bubbly liquid:

$$\text{Re} = \frac{\Omega a(b - a)}{\nu} = \frac{\Omega a(b - a)}{\nu_0(1 + \tfrac{5}{2}\alpha)}. \qquad (4)$$

Altogether, we had four different experimental settings: smooth walls with single-phase liquid, smooth walls with two-phase liquid, rough walls with single-phase liquid, and rough walls with two-phase liquid. The Reynolds number range spans $1 \times 10^5 < \text{Re} < 4 \times 10^5$, which is limited by the maximum available torque of the motor.

The experimental procedure was as follows: We first measured the dimensionless drag without bubble injection as a function of the Reynolds number, $c_\epsilon(\alpha = 0, \text{Re})$. The resulting data are fitted by a spline or in the smooth-wall case by a crossover function [6,32], leading to two curves $c_\epsilon^{\text{fit}}(\alpha = 0, \text{Re})$, namely, one for the smooth-wall case [shown in the inset in Fig. 1(a)] and one for the rough-wall case. We then kept the rotation rate of the inner cylinder constant and slowly increased the void fraction while continuously measuring both α and the torque.

In Fig. 1(a), we show the compensated drag coefficient $c_\epsilon(\alpha, \text{Re})/c_\epsilon^{\text{fit}}(0, \text{Re})$ vs the Reynolds number for increasing void fractions α for the smooth-wall case. Once α exceeds a threshold of about 2% volume concentration, a strong drag reduction of up to 25% can be observed, as compared to the single-phase case.

For the rough-wall case, the behavior is very different, as can be seen from Fig. 1(b). In contrast to the smooth-wall case, the drag coefficient increases with increasing void fraction α, even up to 16% for the 8% void fraction case. We conclude that the wall roughness prevents bubbly drag reduction. Apparently, drag reduction by bubbles is a boundary layer effect, just as polymeric drag reduction [26]: In the rough-wall case, the structure of the viscous BLs and, thus, the energy injection mechanism into the system seem to be so strongly modified that the mechanism for bubbly drag reduction can no longer be active.

We point the reader to some interpretation ambiguities on what drag reduction means. In Fig. 2, we present the
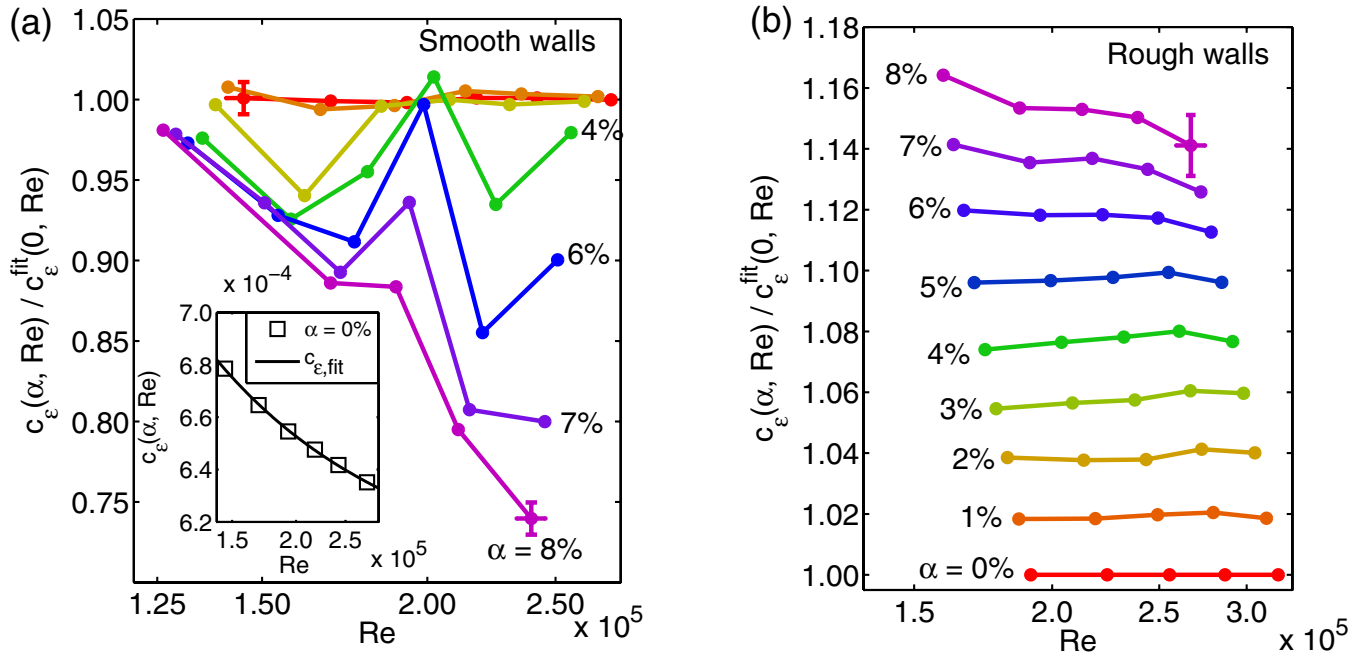
FIG. 1 (color online).   Compensated drag coefficient $c_\epsilon(\alpha, \mathrm{Re})/c_\epsilon^{\mathrm{fit}}(0, \mathrm{Re})$ vs the Reynolds number for increasing void fractions α for (a) the smooth-wall case and (b) the rough-wall case. While (a) in the smooth-wall case, the drag decreases up to 25%, (b) in the rough-wall case, the bubble injection leads to a drag enhancement.

data for the rough- and smooth-wall cases in their *dimensional* form. For the smooth-wall case [Fig. 2(a)], with increasing void fraction a reduction in the required torque for constant rotation rate is observed, just as expected. However, in the rough-wall case [Fig. 2(b)], the dimensional torque does not seem to depend on the (increasing)

void fraction. This means that only when compensating for the change in density and viscosity can the rough-wall results be interpreted as drag increase through bubble injection. The smooth-wall case is free of this interpretation ambiguity: Both the dimensional and the dimensionless drag decrease with increasing void fraction α.
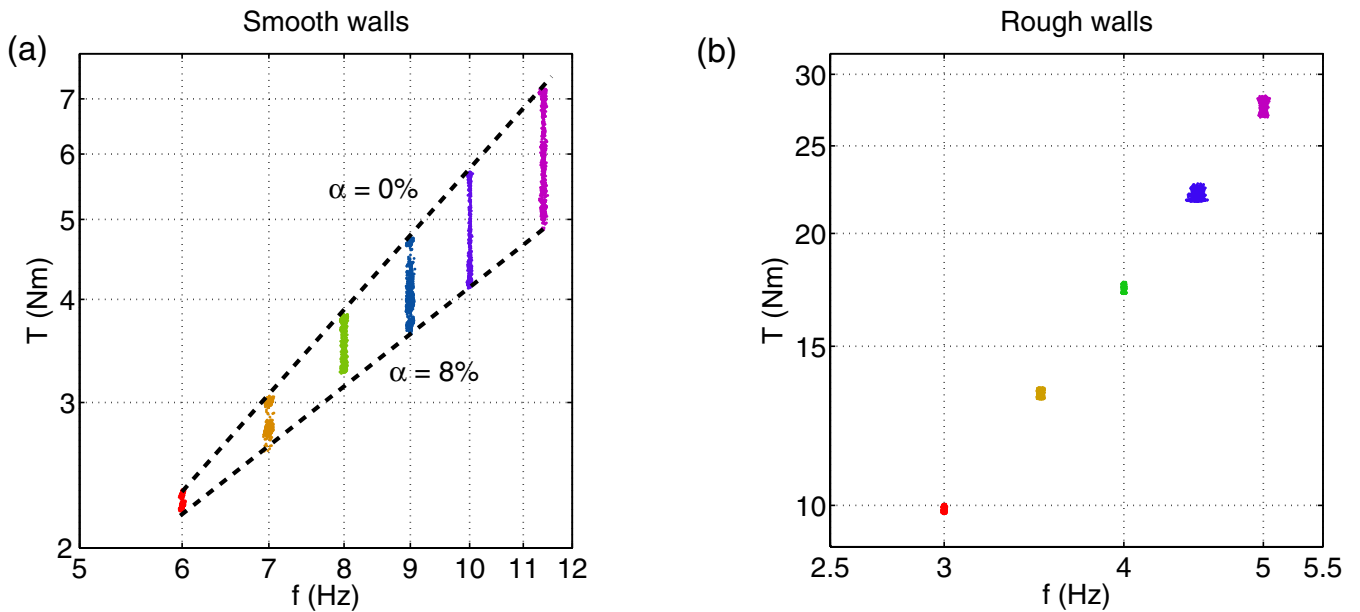
FIG. 2 (color online).   Torque (in Nm) versus the rotation rate (in hertz) of the inner cylinder for increasing void fractions: (a) - smooth-wall case and (b) rough-wall case. In (a), a decrease of dimensional torque with increasing void fraction α can be seen. In (b), the dimensional torque seems to be independent of the void fraction.

In order to compare our results with theoretical approaches [19], it would be of prime interest to know the bubble concentration profile, both in the smooth- and in the rough-wall cases. For low Re, such measurements have been done, revealing a strong Re dependence of the radial bubble distribution [33]. Corresponding measurements in the large Re case are on their way.

In conclusion, we have measured the drag for bubbly turbulence in a Taylor-Couette system for smooth and rough walls. For the smooth-wall case, a strong reduction in drag coefficient was found, in agreement with our earlier experimental results [6] and in agreement with theory [19]. For the rough-wall case, we found an enhancement of the dimensionless drag coefficient with increasing void fraction, whereas the dimensional torque did not change. Independent of these interpretation ambiguities, the general conclusion is quite clear: There is no drag reduction for Taylor-Couette turbulence with rough walls—at least not in the (Taylor-)Reynolds number regime accessible in our experiments—whereas a strong drag reduction is observed for the smooth-wall case. Bubbly drag reduction is, hence, a boundary layer effect.

Through our results, one can understand why growth of barnacles or other organic material at the ship hull or its corrosion drastically degrade the drag reduction effect of injected bubbles: The roughness caused by the organic material or by the corrosion destroys the smooth BL and, therefore, the mechanism leading to bubbly drag reduction.

---

*Electronic address: d.lohse@utwente.nl

[1] P. S. Virk, AIChE J. **21**, 625 (1975).

[2] N. S. Berman, Annu. Rev. Fluid Mech. **10**, 47 (1978).

[3] R. Benzi, E. S. C. Ching, N. Horesh, and I. Procaccia, Phys. Rev. Lett. **92**, 078302 (2004).

[4] V. S. L'vov, A. Pomyalov, I. Procaccia, and V. Tiberkevich, Phys. Rev. Lett. **92**, 244503 (2004).

[5] S. Pal, S. Deutsch, and C. L. Merkle, Phys. Fluids A **1**, 1360 (1989).

[6] T. H. van den Berg, S. Luther, D. P. Lathrop, and D. Lohse, Phys. Rev. Lett. **94**, 044501 (2005).

[7] J. Xu, M. R. Maxey, and G. E. Karniadakis, J. Fluid Mech. **468**, 271 (2002).

[8] K. Sugiyama, T. Kawamura, S. Takagi, and Y. Matsumoto, in *Proceedings of the 4th Symposium on Smart Control of Turbulence* (University of Tokyo, Tokyo, 2003); in *Proceedings of the 5th Symposium on Smart Control of Turbulence* (University of Tokyo, Tokyo, 2004), pp. 31–43, www.turbulence-control.gr.jp/PDF/symposium/FY2003/Sugiyama.pdf.

[9] N. K. Madavan, S. Deutsch, and C. L. Merkle, Phys. Fluids **27**, 356 (1984); J. Fluid Mech. **156**, 237 (1985).

[10] C. Merkle and S. Deutsch, in *Frontiers in Experimental Fluid Mechanics*, edited by M. G. el Hak, Lect. Notes Eng. Vol. 46 (Springer, Berlin, 1989), p. 291.

[11] V. S. L'vov, A. Pomyalov, I. Procaccia, and V. Tiberkevich, Phys. Rev. Lett. **94**, 174502 (2005).

[12] W. C. Sanders *et al.*, J. Fluid Mech. **552**, 353 (2006).

[13] S. Deutsch *et al.*, J. Fluid Mech. **556**, 309 (2006).

[14] Y. Kodama, A. Kakugawa, T. Takahashi, and H. Kawashima, Int. J. Heat Fluid Flow **21**, 582 (2000).

[15] Y. Kodama, A. Kakugawa, S. Nagaya, and T. Kawamura, Report of the 24th U.S.-Japan Joint Meeting, Marine Facilities Panel of the U.S./Japan Cooperative Program in Natural Resources, 2001 (unpublished).

[16] R. Latorre, A. Miller, and R. Philips, Trans. Soc. Nav. Arch. Mar. Eng. **110**, 259 (2002).

[17] A. Ferrante and S. Elghobashi, J. Fluid Mech. **503**, 345 (2004).

[18] J. C. Lu, A. Fernandez, and G. Tryggvason, Phys. Fluids **17**, 095102 (2005).

[19] T. S. Lo, V. S. L'vov, and I. Procaccia, Phys. Rev. E **73**, 036308 (2006).

[20] T. H. van den Berg, C. Doering, D. Lohse, and D. P. Lathrop, Phys. Rev. E **68**, 036307 (2003).

[21] O. Cadot *et al.*, Phys. Rev. E **56**, 427 (1997).

[22] S. Grossmann and D. Lohse, J. Fluid Mech. **407**, 27 (2000); Phys. Rev. Lett. **86**, 3316 (2001); Phys. Rev. E **66**, 016305 (2002); Phys. Fluids **16**, 4462 (2004).

[23] B. Eckhardt, S. Grossmann, and D. Lohse, Eur. Phys. J. B **18**, 541 (2000); Europhys. Lett. (to be published).

[24] S. Deutsch, M. Moeny, A. A. Fontaine, and H. Petrie, Exp. Fluids **37**, 731 (2004).

[25] M. Vlachoginannis and T. J. Hanratty, Exp. Fluids **36**, 685 (2004).

[26] O. Cadot, D. Bonn, and S. Douady, Phys. Fluids **10**, 426 (1998).

[27] R. Benzi *et al.*, J. Fluid Mech. **551**, 185 (2006).

[28] D. P. Lathrop, J. Fineberg, and H. S. Swinney, Phys. Rev. Lett. **68**, 1515 (1992); G. S. Lewis and H. L. Swinney, Phys. Rev. E **59**, 5457 (1999).

[29] F. Risso and J. Fabre, J. Fluid Mech. **372**, 323 (1998).

[30] A. Einstein, Ann. Phys. (Berlin) **324**, 289 (1906).

[31] A. Acrivos, J. Rheol. (N.Y.) **39**, 813 (1995).

[32] D. Lohse, Phys. Rev. Lett. **73**, 3223 (1994).

[33] Y. Murai, H. Oiwa, and Y. Takeda, J. Phys.: Conf. Ser. **14**, 143 (2005).